



# HHS Public Access

Author manuscript

*Cancer Lett.* Author manuscript; available in PMC 2019 December 02.

Published in final edited form as:

*Cancer Lett.* 2018 September 28; 432: 216–226. doi:10.1016/j.canlet.2018.06.011.

## Nrf2-activated expression of sulfiredoxin contributes to urethane-induced lung tumorigenesis

Murli Mishra<sup>a</sup>, Hong Jiang<sup>a,b</sup>, Hedy A. Chawsheen<sup>a</sup>, Matthieu Gerard<sup>c</sup>, Michel B. Toledano<sup>d</sup>, Qiou Wei<sup>a,b,\*</sup>

<sup>a</sup>Department of Toxicology and Cancer Biology, University of Kentucky, Lexington, KY, 40536, USA

<sup>b</sup>Markey Cancer Center, University of Kentucky, Lexington, KY, 40536, USA

<sup>c</sup>Epigenetic Regulation and Cancer Group, Institut de Biologie et de Technologies de Saclay (iBiTecS), CEA-Saclay, 91191, Gif-sur-Yvette, France

<sup>d</sup>Oxidative Stress and Cancer Group (LSOC), Institut de Biologie et de Technologies de Saclay (iBiTecS), CEA-Saclay, 91191, Gif-sur-Yvette, France

### Abstract

Lung cancer is the leading cause of cancer death worldwide. Cigarette smoking and exposure to chemical carcinogens are among the risk factors of lung tumorigenesis. In this study, we found that cigarette smoke condensate and urethane significantly stimulated the expression of sulfiredoxin (Srx) at the transcript and protein levels in cultured normal lung epithelial cells, and such stimulation was mediated through the activation of nuclear related factor 2 (Nrf2). To study the role of Srx in lung cancer development *in vivo*, mice with Srx wildtype, heterozygous or knockout genotype were subjected to the same protocol of urethane treatment to induce lung tumors. By comparing tumor multiplicity and volume between groups of mice with different genotype, we found that Srx knockout mice had a significantly lower number and smaller size of lung tumors. Mechanistically, we demonstrated that loss of Srx led to a decrease of tumor cell proliferation as well as an increase of tumor cell apoptosis. These data suggest that Srx may have an oncogenic role that contributes to the development of lung cancer in smokers or urethane-exposed human subjects.

### Keywords

Oxidative stress; Antioxidant; Signal transduction; Cell growth and proliferation; Peroxiredoxins

---

\*Corresponding author. Department of Toxicology and Cancer Biology, University of Kentucky, Lexington, KY, 40536, USA. qiou.wei@uky.edu (Q. Wei).

Conflicts of interest  
None to declare.

## 1. Introduction

Lung cancer is the most commonly diagnosed cancer and the leading cause of cancer-related mortality in the United States and worldwide. With more than 50 histological variants, lung cancer is extremely heterogeneous and lung adenocarcinoma accounts for more than 40% of its overall incidence. Although significant progress has been made over the past decade in the early detection and chemotherapeutic treatment of lung cancer, the five-year survival rate of patients with stage IV non-small cell lung cancer is less than 1% [1]. Cigarette smoking and exposure to chemical carcinogens are among the risk factors of lung cancer development in humans [2]. Understanding the cell signaling pathways that are activated by cigarette smoke and chemical carcinogens may facilitate the development of effective strategies to prevent lung tumorigenesis in smokers and to enforce targeted cancer therapeutics in patients.

Molecular mechanisms of lung cancer development are very complicated and are far from fully understood. One major challenge is the complexity of the components in cigarette smoke. It contains more than 4000 chemicals and many of them are known to play a role in cell transformation [3]. Exposure of lung epithelium to cigarette smoke causes various damages, which are at least partially resulted from the production of reactive oxygen species and reactive nitrogen species, such as superoxide, hydrogen peroxide, hydroxyl radical, and peroxynitrite [4–6]. The accumulation of these species leads to oxidative stress that not only damages DNA, RNA and proteins but also activates oncogenic signaling pathways. As a result, exposure to cigarette smoke or other chemical carcinogens leads to increased frequency of genetic mutations and facilitates cell transformation that results in uncontrolled cell growth. The proliferation of mutated cells eventually leads to the formation of tumor mass. Therefore, understanding the mechanism of cellular response to oxidative stress may be beneficial for the development of effective strategies to prevent and/or treat lung cancer in patients.

After exposure to cigarette smoke or chemical carcinogens, lung epithelial cells respond by changing the levels of gene expression to antagonize the deteriorating effect of oxidative stress. Among these changes are the expression of different cellular antioxidant enzymes [7–9]. Whether and how cigarette smoke-induced antioxidants are involved in lung tumorigenesis and their role in oncogenic signaling are not well understood. In this study, we used cultured human lung epithelial cells, genetically engineered mouse as well as a model of urethane-induced lung tumorigenesis to investigate the functional significance of redox proteins, including sulfiredoxin (Srx) and peroxiredoxin (Prx) in lung tumorigenesis. We found that exposure of human lung epithelial cells to cigarette smoke condensate (CSC) or urethane activates the expression of Srx and certain Prxs. Such activation is mediated through the nuclear related factor 2 (Nrf2)-dependent transcriptional activation mechanism. In the urethane-induced mouse lung tumorigenesis model, we found that depletion of Srx led to reduced tumor multiplicity and smaller volume in Srx knockout mice. Taken together, our study demonstrated that increased expression of Srx may contribute to lung cancer development in smokers or urethane exposed human subjects, and strategies of targeting Srx may be used as promising methods for the treatment of lung cancer in patients.

## 2. Materials & methods

### 2.1. Cell culture, chemicals, antibodies and western blotting

Human lung/bronchus normal epithelial BEAS2B cell line was commercially obtained from American Type Culture Collection (Manassas, VA). Cells were authenticated by DNA fingerprinting with a polymerase chain reaction (PCR) -based short tandem repeat profiling, which confirmed that the BEAS2B cell line used in this study was originated from a single source and was not contaminated by other cell lines. In addition, cells in culture were periodically examined by fluorescence imaging using Hoechst 33258 to ensure that all cells were free of mycoplasma infection. Cells were cultured in BEGM™ Bronchial Epithelial Cell Growth Medium Culture medium containing various supplements (Lonza Inc., Walkersville, MD). All cells were cultured under strictly controlled temperature, humidity and CO<sub>2</sub> conditions as recommended by the cell provider. Experiments were completed using cells within 10 passages of the original ATCC source.

CSC was provided by Dr. Chandra Gary Gairola (University of Kentucky). It was prepared using the University of Kentucky Reference 3R4F cigarettes and has been previously tested and used in multiple studies [10–13]. Urethane was commercially obtained from Sigma-Aldrich (St. Louis, MO). K27 (*N*-[7-chloro-2-(4-fluorophenyl)-4-quinazoliny]-*N*-(2-phenylethyl)- $\beta$ -alanine), a specific inhibitor of Srx [14], was synthesized by AMRI (Albany, NY) through a commercial contract and the purity was verified by HPLC and NMR analysis. Unless otherwise specified, cultured BEAS2B cells were administered with CSC, urethane or other reagent for a period of 48 h before being harvested to measure the levels of mRNA or protein expression. For long-term exposure, cultured cells were treated with indicated concentration of urethane for 5 days. During this course, culture medium was changed every other day with freshly supplemented urethane.

For western blot, cells were harvested and lysed in radio-immunoprecipitation assay buffer containing 50 mM Tris at pH 7.4, 150 mM NaCl, 1% NP-40, 1 mM EDTA, 0.25% sodium deoxycholate, 0.6 mM PMSF and a mixture of 1% protease cocktail inhibitors (Santa Cruz Biotech, Dallas, TX). Protein bands were separated using sodium-dodecyl sulfate-polyacrylamide gel electrophoresis and western blotting was performed following the standard protocol. Briefly, the membrane was blocked for 1 h with 5% nonfat dry milk in tris buffer before an overnight incubation with primary antibody diluted in 5% milk. The membrane was then washed with tris-buffered saline and incubated for 1 h with the horseradish peroxidase-conjugated secondary antibody. After multiple washing steps, the signal was detected using western dura chemiluminescence substrate (ThermoFisher, Waltham, MA) and bands were visualized onto X-ray film. Primary antibodies were anti-Srx (Proteintech, Chicago, IL), anti-PrxSO<sub>2</sub> (Adipogen International), anti-Prx1 (Abcam, Cambridge, MA), anti-Prx2, anti-Prx3 and anti-Nrf2 (Santa Cruz Biotech), anti-Prx4 (Abcam), anti-p-c-Jun (Cell Signaling, Billerica, MA) and anti- $\beta$ -actin (Sigma–Aldrich). All western blotting experiments were repeated independently at least 3 times. For data collection and analysis, relative intensities of bands were quantitated using ImageJ software and data were presented as ratio to  $\beta$ -actin under the same conditions (the ratio of control to its  $\beta$ -actin was set to 1 and other ratios were adjusted proportionally).

## 2.2. Regular reverse transcription polymerase chain reaction (RT-PCR) and quantitative real-time PCR (qRT-PCR)

After treatment as specified, total RNA was extracted from cultured cells using the RNeasy Kit (Qiagen, Valencia, CA). About 50 ng of purified RNA was used as template, and cDNA was made by M-MuLV reverse transcriptase using the first strand cDNA synthesis kit (Invitrogen) following the manufacturer's suggested protocol. Newly synthesized cDNA was further purified and used in regular RT-PCR and qRT-PCR for quantification. Primer pairs used in these reactions were specific for genes in mouse, including Srx forward 5'-AAAGTGCAGAGCCTGGTGG-3' and reverse 5'-CTTGGCAGGAATGGTCTCTC-3'; Nrf2 forward 5'-AGTGGATCTGCCAACTACTC-3' and reverse 5'-CATCTACAAACGGGAATGTCTG-3'; Prx1 forward 5'-ACCTCTTCCTGCGTTCTCAC-3' and reverse 5'-TGTCCATCTGGCATAACAGC-3'; Prx2 forward 5'-GTCCTTCGCCAGATCACTGT-3' and reverse 5'-ACGTTGGGCTTAATCGTGTC-3'; Prx3 forward 5'-GCCGTTGTCAATGGAGAGTT-3' and reverse 5'-TCCACTGAGACTGCGACAAC-3'; Prx4 5'-CAGCTGTGATCGATGGAGAA-3' and reverse 5'-ATCCTTATTGGCCCAAGTCC-3'; GAPDH forward 5'-ACAACTTTGGCATTGTGGAA-3' and reverse 5'-GATGCAGGGATGATGTTCTG-3'.

All primers were used at a final concentration of 1  $\mu$ M in the PCR reaction. After the denature at 95 °C for 2 min, PCR reaction was followed by 30 cycles of 95 °C for 15 s, 55 °C for 30 s, and 72 °C for 30 s. For gel analysis of regular RT-PCR, the PCR product was loaded with 6X running buffer in the presence of SYBR green, and the mixture was separated on 3% agarose gel and visualized using the UV imager. Relative intensity of the PCR band was quantitated and normalized to the level of glyceraldehyde-3-phosphate-dehydrogenase (GAPDH) using ImageJ software (version 1.49). For the qRT-PCR assay, each reaction was repeated in six replicates and was carried out in the LightCycler 480 Real-Time PCR System using the plate with SYBR Green Master Mix (Roche Applied Science, Mannheim, Germany). The qRT-PCR reaction was started with 95 °C for 2 min and followed by 35 cycles of 95 °C for 15 s, 55 °C for 30 s and 72 °C for 30 s. The specificity of the reactions was verified by continuous fluorescence measurement that showed an effective dissociation curve between 55 °C and 95 °C. Relative levels of target mRNA were calculated based on the  $2^{-C_t}$  method, and final quantitative results were averaged from six replicates normalized to the mRNA level of GAPDH.

## 2.3. Lentiviral ShRNA knockdown of Srx in BEAS2B cells

Mission-ShRNA control and target gene constructs were commercially obtained from Sigma-Aldrich. Viral particles were made in HEK293T cells following the provider's suggested protocol. Cells were infected with lentiviral particles containing control non-target ShRNA (ShNT) or ShRNA targeting the coding region of Srx mRNA (ShSrx) as previously published [15]. Stable cells were established and maintained in culture medium containing 1.0  $\mu$ g/ml of puromycin.

#### 2.4. Soft agar colony formation assay

BEAS2B cells were pre-treated with 5 mM and 10 mM urethane dissolved in phosphate buffer saline (PBS) for 5 days. Control cells were treated with PBS. Cells were then counted using an automated cell counter and suspended in 0.3% agar diluted with culture medium. About 15,000 cells were plated into each well of the 6-well plate that was pre-coated with 1 ml/well of 0.6% agar. After 24 h, urethane was added to the treatment group and PBS to the control group. There was six replicates in each group of treatment or control. Culture medium was changed on every fifth day, with fresh urethane/vehicle added when the medium was changed. Cells in plates were incubated for 6 weeks. Colonies were stained with 0.25% crystal violet and images were taken using Amscope 3.7 software with a digital camera. The size and number of colonies were counted and analyzed using OpenCFU software (version 3.8.11).

#### 2.5. Mouse breeding, genotyping and urethane-induced lung tumorigenesis protocol

Mouse breeding, genotyping and experimental animal protocol were approved by the *Animal Care and Use Committee* of the University of Kentucky. All procedures in mouse experiments were carried out following the “*PHS Policy on Humane Care and Use of Laboratory Animals*” (NIH publication number 15–8013), and in accordance with the guidelines as described in the book “*Guide for the care and use of laboratory animals*” by the National Institute of Health (NIH publication number 90–23). Srx knockout mouse was generated on FVB background using Srx  $-/-$  B6/129 mouse backcrossed with FVB strain as previously published [16,17]. Genomic DNA from tail clip was extracted using genomic DNA extraction kit (Qiagen); PCR-based genotyping was performed as previously reported [18].

A randomized, double-blind experimental design was applied in mouse experiments to eliminate potential subjective bias. To avoid variation caused by gender difference, only female mice were used in each genotype (15 mice/genotype). Briefly, mice at 7-week of age, including wild type (Wt), heterozygous, and knockouts, were given intraperitoneal injection of 1 mg/g body weight of urethane dissolved in saline. Injection was carried out once weekly for 3 weeks. After injection, all mice were maintained on a normal diet and water *ad libitum* for 10 weeks. During this period, mice were monitored for general health including water, food intake and body weight. At the end of 10 weeks, all mice were humanely euthanized. Mouse lungs were perfused with PBS, extracted, and rinsed at least three times in sterile PBS. Tumors on the surface of the lung were examined and measured under a dissection scope. To visualize microscopic tumors, mouse lungs were fixed in 4% paraformaldehyde and stored in 70% ethanol before being processed through standard paraffin embedding and sectioning. For histological assessment, lobes from each lung were sequentially sectioned for a total of 15 slides. Slides were stained for hematoxylin and eosin (H&E) to measure the number and size of tumors under dissecting or low-magnification scope.

#### 2.6. Immunohistochemistry staining for cell proliferation and apoptosis assay

Tissue slides collected from a representative group of five mice in each genotype were used for staining. Immunohistochemistry was performed using Vectastain Elite ABC kit #PK-6100 (Vector Laboratories, Inc., Burlingame, CA). For cell proliferation assay, slides

were stained with anti-Ki67 (1:50, Abcam, Cambridge, MA). For apoptosis, terminal deoxynucleotidyl transferase-mediated dUTP nick end labeling (TUNEL) staining was performed using TACS 2TdT-DAB In Situ Apoptosis Detection Kit (Trevigen, Gaithersburg, MD). Methyl green was used as counterstaining. Slides were dehydrated, mounted before visualizing under the Zeiss Axioplan 2 microscope (Carl Zeiss Microscopy, LLC, Thornwood, NY). For quantification, images were obtained using the Aperio slide scanning system and relative staining intensity was measured using the ImageScope software with color deconvolution algorithms (version 11.2.0.780).

## 2.7. Statistical analysis

Quantitative data were presented as mean  $\pm$  standard deviation ( $\bar{x} \pm SD$ ). Data were analyzed in GraphPad Prism (version 6.01) using appropriate statistical methods such as the student *t*-test, paired *t*-test, one way or two-way analysis of variance (ANOVA) as specified in each result. The *p*-value was calculated using a two-tailed 95% confidence interval and the *p*-value of 0.05 was considered statistically significant.

## 3. Results

### 3.1. Exposure of BEAS2B cells to CSC activated the expression of Srx

To study the effect of CSC on the expression of Srx, BEAS2B cell line was used in this study. It was established and immortalized from human lung normal epithelium, and was widely used to study the response of lung epithelial cells to various environmental and genetic challenges. CSC was prepared from standard cigarette extracts and it contained the majority of chemicals and carcinogens that were found in cigarette smoke [10,19]. Therefore, treatment of cells in culture with CSC can be used in the laboratory to mimic the exposure of lung epithelial cells to cigarette smoke in human. After treatment of BEAS2B cells with CSC at the concentrations of 10, 20 and 40  $\mu\text{g}/\text{mL}$  for 48 h, we observed a dose-dependent increase of Srx protein expression by western blotting (Fig. 1A and B). The typical 2-Cys containing Prxs, including Prx1 ~ 4, are considered as specific substrates of Srx [20]. Therefore, we also examined the effect of CSC on their levels of expression. We found significantly increased expression of Prx1, 2 and 4 in CSC-treated cells, especially in those treated with 40  $\mu\text{g}/\text{ml}$  of CSC (compared with control,  $p < 0.05$ , *t*-test). A slightly increased level of Prx3 was also observed but such change was not statistically significant. To determine whether the increased levels of Srx and Prxs were resulted from the activation in gene transcription, we extracted total RNA from control and CSC-treated cells. Both traditional reverse transcriptase-PCR (RT-PCR) (Fig. 1C and D) and qRT-PCR (Fig. 1E) were used to measure the levels of Srx/Prxs transcripts, and we found significant increases in the mRNA levels of Srx, Prx1, 2 and 4 in CSC-treated cells. These data indicate that CSC upregulates the expression of Srx and certain members of the Prxs through the activation of gene transcription.

### 3.2. Treatment of BEAS2B cells with urethane activated the expression of Srx and Prxs

Next we asked whether Srx and Prxs can be activated by other known risk factors of lung cancer. Chemical carcinogens, such as urethane, have been known to cause lung cancer development in humans as well as rodents. Therefore, BEAS2B cells were treated with



urethane at the dose of 5 and 10 mM for 5 days. Cell lysates were then collected and subjected to Western blotting. We found a significant, dose-dependent increase of Srx, Prx1 and Prx2 in urethane treated cells (Fig. 2A and B). In contrast, the changes on protein levels of Prx3 and Prx4 were not as significant as observed in cells treated with CSC. Further qRT-PCR analysis demonstrated that such increases at the protein level of Srx, Prx1 and Prx2 were also correlated significantly with their increases at mRNA level (Fig. 2C). Therefore, the activation of Srx, Prx1 and Prx2 by urethane was also mediated through a transcriptional activation mechanism. Taken together, our data indicate that exposure of human lung normal epithelial cells to CSC or urethane can activate the expression of Srx and certain members of the Prxs through the activation of gene transcription.

### 3.3. Urethane stimulated the expression of Srx and Prx1 through the activation of Nrf2

In our previous studies [15,21,22], we have demonstrated that Srx enhances lung cancer development through the interaction/activation of Prx1 and Prx4; whereas the expression of Prx2 or Prx3 has marginal contribution since targeted depletion (or overexpression) of Prx2 or Prx3 has no significant effect on lung cancer cell malignancy. Based on those studies, we believe that the increased expression of Prx2 will not contribute significantly to lung tumorigenesis or cancer progression, although its expression was stimulated by CSC and urethane. Our following efforts were thus focused on the understanding of how urethane stimulated the expression of Srx and Prx1. Among all transcription factors, it has been well demonstrated that the activation of activator protein 1 (AP-1) or nuclear related factor 2 (Nrf2) stimulates the expression of Srx through binding to the proximal promoter [21,23,24]. Among these factors, c-Jun is one of the major components of the AP-1 complex that activates Srx gene transcription. After treatment of BEAS2B cells with urethane, we found no significant changes either at the level of total c-Jun or its activated form as indicated by western blotting. However, we identified a dose-dependent increase of Nrf2 protein upon urethane treatment (Fig. 3A and B). Trigonelline, a coffee-derived alkaloid, is a chemical inhibitor that represses Nrf2-mediated downstream target gene activation through blocking the translocation of Nrf2 from cytoplasm to nuclear [25,26]. After treatment of BEAS2B cells with urethane in the presence or absence of trigonelline, we found that trigonelline did not inhibit urethane-induced expression of Nrf2 at the protein level, but it significantly inhibited the expression of Srx and Prx1 under the same conditions (Fig. 3C and D). Presumably, this was due to the inhibition of Nrf2 activity by trigonelline. Taken together, these data suggest that urethane-induced expression of Srx and Prx1 is mediated, at least partially, through a mechanism of Nrf2-dependent transcriptional activation.

### 3.4. Expression of Srx contributed to urethane induced BEAS2B cell transformation

Anchorage-independent colony growth is a hallmark of cell transformation and is an *in vitro* model that strongly correlates with tumorigenicity *in vivo* [27,28]. We then asked whether treatment of BEAS2B cells by urethane led to cell transformation through the measurement of anchorage independent colony growth under different conditions. BEAS2B cells were cultured in soft agar and urethane was added to the culture medium periodically. As indicated in Fig. 4A, compared with vehicle treated control group, there was a significant increase of colonies in soft agar in cells treated with urethane. A higher concentration of urethane treatment led to the formation of more colonies. To study whether Srx was required

for urethane-induced colony formation, control ShNT or ShSrx was transfected into BEAS2B cells by viral infection and stable cells were established by antibiotic selection. As verified by western blot, the expression of ShSrx completely abolished urethane-induced expression of Srx in BEAS2B cells (Fig. 4B). When grown in soft agar, there was a significant decrease of colonies in ShSrx cells compared with ShNT cells, despite the same treatment of urethane in both cells (Fig. 4C). To further explore whether the enzymatic activity of Srx is required for the colony formation, a specific inhibitor of Srx named K27 was used in our study. Treatment of BEAS2B cells with K27 abolished the ability of Srx to reduce the hyperoxidized Prxs in urethane treated cells (Fig. 4D). It also significantly inhibited the growth of soft agar colonies that were induced by urethane (Fig. 4E). These data demonstrate that depletion of Srx or inhibition of its activity represses urethane-induced anchorage-independent colony growth of BEAS2B cells, suggesting that expression of Srx is likely a contributing factor that promotes urethane-induced lung epithelial cell transformation.

### 3.5. Srx knockout mice were resistant to urethane-induced lung tumorigenesis

Srx knockout mice were established in FVB background, and these mice were completely normal under laboratory conditions [16,18]. To study the role of Srx in lung cancer *in vivo*, we carried out a well-established urethane-induced mouse lung tumorigenesis protocol [29,30]. In this model, it has been previously demonstrated that gender is a potential variation factor due to different susceptibility of male and female mouse to urethane [31–33]. To exclude such variation and reduce the work load, only female mice (15 mice/group) with either Srx wildtype, heterozygote or knockout were used in our study. As indicated in Fig. 5A, each mouse was given a weekly dose of urethane (1.0 mg/g body weight) for 3 weeks by intraperitoneal injection. Mice were maintained for a total of 10 weeks before being humanely euthanized.

Loss-of-body weight is a non-invasive sign that indicates the development of tumors, and is often used to monitor tumor severity in the mouse model of chemical carcinogenesis [30]. In our study, we examined mouse body weight weekly before and after urethane treatment, and found that Srx knockout and heterozygous mice showed significantly more gain of body weight compared with the group of wildtype ( $p < 0.001$ ). However, the weight difference between groups of heterozygous and knockout mouse was not statistically significant ( $p = 0.148$ ) (Fig. 5B). The slower rate of weight gain in Srx wildtype group may thus indicate more tumor development caused by urethane. To confirm this, all mice were humanely sacrificed and lungs were extracted at the end of the tenth week. As shown by the gross imaging (Fig. 5C), tumor nodules were observed in every mouse that had been treated with urethane, regardless of their genotypes. H&E staining and histopathology examination indicated that tumors had typical histological features of lung adenocarcinoma (Fig. 5D). These data suggest that FVB mice are sensitive to urethane treatment, and loss of Srx does not affect the overall incidence of mice with lung tumors in each group.

To further quantitate the multiplicity and volume of lung tumors in each group of mice, we did sequential sectioning and H&E staining on each lobe of the mouse lung. The number and diameter of tumors were counted and measured under dissecting scope or low-



magnification microscope. We found that the average number of tumors per lung in Srx knockout group was approximately 50% of those observed in the wildtype, indicating a two-fold reduction of tumor multiplicity resulting from the loss of Srx (Fig. 5E). The average diameter of tumors in Srx knockout mice was also significantly smaller than those of wildtype (Fig. 5F). Although a trend of decrease in tumor number and diameter was observed in Srx heterozygote, such difference was not statistically significant when compared with those of wildtype ( $p = 0.199$  and  $p = 0.174$ , respectively). Taken together, our data suggest that depletion of Srx renders mice resistant, at least partially, to urethane-induced lung tumorigenesis. However, loss of Srx alone is not able to prevent the formation of lung tumors induced by urethane in this mouse model.

### 3.6. Urethane activated the expression of Srx, Prx1 and Nrf2 in mouse lung tumors and normal adjacent tissue

From cell culture studies we found that the levels of Srx and Prx1 were significantly induced by urethane, and their induction was due to an increased expression of Nrf2-mediated gene transcription. Next we asked whether such effects of urethane on these proteins were also true *in vivo*. Tumor slides from a group of five representative mice were stained for Srx, Prx1 and Nrf2 using authenticated, specific antibodies. Since Srx was depleted at the genomic level, anti-Srx staining in both tumors and adjacent normal tissue in the lungs of knockout mice were shown as background, negative staining. However, strongly positive anti-Srx staining (shown as dark brown) was observed in both tumors and adjacent normal tissue in the lungs of wildtype as well as heterozygous mice (Fig. 6A). In anti-Prx1 (Fig. 6B) and anti-Nrf2 staining (Fig. 6C), tumor cells and adjacent normal tissue from all mice were stained positive regardless of their phenotypes. After comparing the intensity of staining, we found no significant difference on the average levels of Srx, Prx1 or Nrf2 between tumors of different genotypes (bar graphs in Fig. 6B and C). Therefore, consistent with our data obtained in cell culture studies, treatment of urethane in wildtype mice led to increased expression of Srx, Prx1 and Nrf2 in both tumors and normal adjacent tissue, and loss of Srx alone did not significantly affect the expression of Prx1 or Nrf2 induced by urethane.

### 3.7. Depletion of Srx inhibited cell proliferation and increased apoptosis in urethane-induced mouse lung tumors

To understand why Srx knockout mouse under same protocol of urethane treatment had reduced tumor multiplicity and smaller volume, we examined the rate of cell proliferation and apoptosis in tumors from different genotypes. Ki67 is a nuclear protein that is associated with ribosomal RNA transcription, and is often used as a specific indicator of cell proliferation. As shown in Fig. 7A, most nuclei (more than 60% of tumor cells) in tumors from wildtype mice were intensely stained positive for Ki67, whereas fewer cells in tumors from either Srx +/- or Srx -/- mice were stained positive. After quantitation and statistical analysis, we found that tumors from Srx +/- or Srx -/- mice had significantly lower staining of Ki67 than those of Srx +/+ tumors (Fig. 7A bar graph). These data indicate that depletion of Srx significantly decreases the rate of tumor cell proliferation. In principle, the formation of a tumor mass is not only resulted from increased rate of cell proliferation, but also reversely correlated with the rate of cell death. We then examined the amount of apoptotic cells in these tumors using TUNEL assay. As shown in Fig. 7B, the majority (> 95%) of

tumor nuclei in Srx  $+/+$  tumors was stained negative, except few cells were stained as positive (shown as dark black staining). However, a significant portion ( $> 20\%$ ) of tumor cells in Srx  $-/-$  tumors were TUNEL positive. Quantitatively, the intensity of TUNEL positive staining was significantly higher in Srx  $-/-$  tumors compared with those in tumors from either Srx  $+/-$  or Srx  $+/+$  mice. When compared tumors of Srx  $+/-$  with those of Srx  $+/+$ , a trend of lower intensity in Srx  $+/+$  tumors was observed, but such difference was not statistically significant. Taken together, reduced cell proliferation and increased apoptosis resulting from the loss of Srx may lead to the decrease of tumor multiplicity and smaller volume in Srx knockout mice.

#### 4. Discussion

Cellular antioxidants, such as glutaredoxin, Prx, thioredoxin, and thioredoxin-like proteins, have been identified as overexpressed in different types of tumors including lung cancer. How these antioxidants contribute to cigarette smoke or chemical carcinogens induced lung cancer development is not completely understood. Among these, Prxs are the major cellular antioxidants that have peroxidase activity. They mediate redox signaling through the formation of intramolecular disulfide bond under physiological conditions; whereas under oxidative stress conditions they scavenge hydrogen peroxide through hyperoxidation [34]. Such activity of Prxs transduces multiple intracellular signal pathways that are critical for physiological and pathological functions in mammalian cells [35]. Srx is the unique enzyme that reduces hyperoxidized Prxs. In particular, the enzymatic activity of Srx is specific to typical 2-Cys containing Prxs, including Prx1, 2, 3 and 4 [20,36,37]. Srx is evolutionarily conserved and has been found in most eukaryotes, but is rare in prokaryotes with few exceptions (e.g. cyanobacteria). To reduce hyperoxidized Prxs back to their active form, Srx utilizes ATP and magnesium as cofactors. The catalytic reaction of Srx is initiated through the formation of sulfinic phosphoryl ester and followed by the production of thiosulfinate intermediate [36,38]. Although previously we have demonstrated a critical role of the Srx-Prx axis in promoting lung cancer cell invasion and metastasis, its role in lung tumorigenesis has not been well studied.

Cigarette smoking is a known factor that causes lung cancer in human. Many chemicals and carcinogens found in cigarette smoke can directly damage human genome through the formation of DNA adducts or modify DNA bases through the accumulation of reactive oxygen species. Due to the complexity of the chemical component of cigarette smoke, it's almost impossible to dissect the oncogenic contribution of every single chemical. To simply the study and data interpretation, we used CSC that was developed in house from reference cigarettes using the established protocol. However, it is worth to point out that CSC may not contain exactly the same chemical components or at equal concentrations as those found in cigarette smoke. Nevertheless, the majority of putative carcinogens found in cigarette smoke are also present in CSC and can be directly detected by high-resolution nuclear magnetic resonance spectroscopy or through additional over-spiking experiments [19]. Therefore, it is reasonable to believe that similar patterns of increased expression in Srx and Prxs may be found in human subjects that have been exposed to cigarette smoke or urethane. In the future, studying the direct effect of cigarette smoke or urethane on the expression of Srx and

Prxs in humans may be useful by providing further evidence to define their role in tobacco-related lung tumorigenesis.

In addition to cigarette smoking, occupational and environmental exposure to chemical carcinogens also contribute significantly to the occurrence and mortality of human lung cancer [39]. Urethane is a chemical carcinogen used as a sedative in patients decades ago, and it is also found at low levels in many foods and byproduct of fermentation. For example, many alcohol and beverage products consumed by humans contain trace amount of urethane and are potential sources of human intake. However, there are separate opinions on whether urethane is present in cigarette smoke and whether or not it is an important contributor to tobacco-related lung cancer [40,41]. Nevertheless, exposure to urethane has been shown to be carcinogenic to humans and rodents, regardless of its source. Mechanistically, urethane itself is not a direct carcinogen that causes genomic mutation. Whereas its metabolite, vinyl carbamate epoxide, is directly toxic to mammalian cells by causing genome instability and DNA mutations [42]. In general, human lung has a very low expression of urethane-metabolizing enzymes prior to the exposure of cigarette smoke or alcohol [43,44]. Consumption of alcohol or smoking increases the expression of urethane-metabolizing enzymes, such as CYP2E1 and esterase, in lung epithelial cells [45]. As a consequence, individuals who consume both alcohol and cigarettes are more likely subjected to increased toxic metabolites of urethane. Indeed, such a population has a higher risk of lung cancer as demonstrated in epidemiological studies of multiple groups [46,47]. With similar etiology and pathogenesis occurring in human, urethane-induced lung carcinogenesis in mouse has been widely used for the mechanistic study of lung cancer.

To conveniently investigate the functional significance of Srx in lung cancer development in the laboratory, cultured BEAS2B cells, CSC and urethane were used in our study. First we examined the effect of CSC on the expression of Srx and different isoforms of Prxs, and found that CSC enhanced the protein expression of Srx and certain Prxs. In addition, we also found that urethane stimulated the expression of Srx and Prx1 through the Nrf2-dependent transcription activation. In BEAS2B cells, urethane-induced cell transformation required the presence and activity of Srx since its knockdown by ShRNA or inactivation by the chemical inhibitor led to the repression of anchorage independent colony formation. Next, utilizing urethane-induced mouse lung tumorigenesis model we found that Srx null mice had significantly reduced tumor multiplicity and smaller volume compared with those of wildtype mice. In mechanistic studies, we revealed that depletion of Srx led to a reduced rate of tumor cell proliferation and increased rate of apoptosis, which collectively contributed to the tumor-resistant phenotype of Srx knockout mice. We have previously shown that increased expression of Srx is not only found in human lung cancer cells, but is also present in the primary tumor specimens of human lung cancer patients [22]. Taken together, our studies reveal a critical, oncogenic role of Srx in lung cancer development. Srx has been discovered as a novel gene preferentially expressed in transformation sensitive mouse skin epithelial cells [48]. We have also demonstrated that Srx is a critical downstream target of tumor promoter induced activator protein 1 (AP-1) activation [21,49]. AP-1 is a dimeric complex that contains members of the Jun, Fos, Atf and Maf transcription factor families. Among these, c-Jun is the central player and a major component of the AP-1 complex. AP-1 activation is well documented as a critical oncogenic pathway that promotes tumorigenesis

and cancer progression, and blocking AP-1 activity has been proposed as therapeutic strategy for the treatment of a variety of human cancer [50,51]. Two AP-1 binding sites have been identified in the Srx gene and both are required for the full activation of its transcription [21]. In addition, an antioxidant response element has also been identified in the proximal region of the Srx gene promoter. Stress factors, including oxidative stress, environmental carcinogens and tumor promoters, can therefore induce Srx expression through increasing the binding of Nrf2 to this element [24,52]. Therefore, to determine the mechanisms that are responsible for the expression of Srx in urethane treated cells, we explored whether treatment of urethane led to the activation of AP-1 and Nrf2. We found no significant changes on the activation of c-Jun after urethane treatment, which suggests that increased expression of Srx by urethane was not directly mediated by AP-1 activation. Furthermore, we found that urethane was able to induce the expression of Nrf2 in human lung epithelial cells, and inhibition of Nrf2 led to the loss of Srx induction.

Studies from others also confirmed that activation of either AP-1 or Nrf-2 pathway was sufficient to stimulate Srx expression [24,53]. In particular, Srx was found to be upregulated in the lungs of mouse exposed to cigarette smoke, and disruption of Nrf2 signaling by genetic knockout in mouse or RNAi in cells inhibited the expression of Srx [52]. In the same study, they also found that expression of Srx protected cells against oxidative stress induced cell death *in vitro*, and loss of Srx was able to sensitize cells to oxidative stress injury. This report is consistent with our current findings that urethane-induced tumors from Srx knockout had significantly increased rate of cell apoptosis, which at least partially contributed to the tumor-resistant phenotype of those mice.

In addition to sensitizing cells to oxidative stress induced cell death, loss of Srx may also lead to the oxidation of mitochondrial lipid that results in apoptosis. In a previous study, Kim et al. identified K27 as a specific inhibitor of Srx enzyme activity, and application of K27 in cultured human lung cancer cells led to a decrease of mitochondria membrane potential, activation of caspase-3 and apoptosis [14]. In particular, this effect of K27 was specific to cancer cells but not to normal lung epithelial cells that had no expression of Srx, and application of K27 *in vivo* significantly inhibited the growth of tumor xenograft in immunodeficient mice. Similar findings were also reported in another study using a different chemical inhibitor of Srx [54]. In our study, we found that K27 was able to inhibit urethane-induced anchorage independent colony growth in BEAS2B cells. In the future, it will be interesting to examine whether the use of Srx chemical inhibitors, such as k27, can prevent or block the formation of lung tumors in experimental mouse models of lung tumorigenesis. Taken together, these studies suggest that targeting Srx may be used as an effective therapeutic strategy for the treatment of lung cancer in patients.

On the other hand, we found that depletion of Srx is not sufficient to prevent or block the formation of tumors in urethane-induced mouse lung tumorigenesis model, suggesting that increased expression of Srx is not likely the driving force that initiates the process of tumorigenesis. Other genes or signaling pathways that are activated by urethane or cigarette smoke may also play a significant role in the initiation of tumorigenesis in this model. For example, it has been demonstrated that early activation of NF- $\kappa$ B signaling and airway inflammation caused by urethane also significantly contribute to lung tumorigenesis in the

FVB mouse [55]. In this study, we found that Nrf2-activated expression of Srx contributed to tumor cell proliferation and survival. Therefore, it is possible that lung tumorigenesis in urethane-induced mouse model results from the activation of both NF- $\kappa$ B and Nrf2 signaling pathways, since inhibition of either alone is not sufficient to render mice free of lung tumors. In our previous studies, we found no correlation between the activation of NF- $\kappa$ B signaling and the expression of Srx [21]. In the future, it is worthwhile to investigate whether inhibition of NF- $\kappa$ B and Nrf2 simultaneously could generate synergistic effect that can completely block tumor formation in urethane-induced mouse lung tumorigenesis model. Moreover, it is not clear whether loss of Srx in mice has any effect on the metabolic process of urethane or affect the mutagenic potential of its metabolites. Furthermore, we found that certain members of the Prx family, such Prx1 and Prx4, were consistently increased in cells or lung tissues treated with urethane. Whether Prx1 or Prx4 plays a role as the “driver” or “passenger” gene in lung tumorigenesis is still unknown. In the future, it will be interesting to study how these members of the Prx family are involved in the process of lung tumorigenesis and how they contribute to the progression of cells from benign adenoma to malignant carcinoma in patients.

In summary, our findings suggest that Srx is one of the oncogenic components that contribute to lung tumorigenesis *in vivo*. In the future, Srx may be considered as a molecular target for precision medicine, and strategies that targeting Srx may have the potential to be used as effective therapeutic methods for the treatment of lung cancer in patients.

## Acknowledgement

We thank Dr. Chandra Gary Gairola (University of Kentucky) for providing CSC; Ms. Heather N. Russell-Simmons, MA, MBA (Research Communication Office, Markey Cancer Center, University of Kentucky), for providing professional editing on the spelling and grammar of the revised manuscript.

### Funding

This work was partially supported by the National Institutes of Health (NCI grant number P30CA177558, R01CA222596), Department of Defense (grant number W81XWH-16-1-0203), American Cancer Society (grant number RSG-16-213-01-TBE) and Kentucky Lung Cancer Research Program 2016.

## Abbreviations:

<b>Srx</b>	Sulfiredoxin
<b>Prx</b>	Peroxiredoxin
<b>Prxs</b>	Peroxiredoxins
<b>AP-1</b>	activator protein 1
<b>Nrf2</b>	nuclear related factor 2
<b>PBS</b>	phosphate buffer saline
<b>CSC</b>	cigarette smoke condensate
<b>ShNT</b>	non-target short hairpin ribonucleic acid

<b>ShSrx</b>	ShRNA targeting Srx
<b>TUNEL</b>	terminal deoxynucleotidyl transferase-mediated dUTP nick end labeling

## References

- [1]. Torre LA, Siegel RL, Jemal A, Lung cancer statistics, *Adv. Exp. Med. Biol* 893 (2016) 1–19. [PubMed: 26667336]
- [2]. Mao Y, Yang D, He J, Krasna MJ, *Epidemiology of lung cancer*, *Surg. Oncol. Clin* 25 (2016) 439–445.
- [3]. Smith CJ, Hansch C, The relative toxicity of compounds in mainstream cigarette smoke condensate, *Food Chem. Toxicol. Int. J. Publ. Br. Ind. Biol. Res. Assoc* 38 (2000) 637–646.
- [4]. Rahman I, MacNee W, Lung glutathione and oxidative stress: implications in cigarette smoke-induced airway disease, *Am. J. Physiol* 277 (1999) L1067–L1088. [PubMed: 10600876]
- [5]. van der Vaart H, Postma DS, Timens W, ten Hacken NH, Acute effects of cigarette smoke on inflammation and oxidative stress: a review, *Thorax* 59 (2004) 713–721. [PubMed: 15282395]
- [6]. Faux SP, Tai T, Thorne D, Xu Y, Breheny D, Gaca M, The role of oxidative stress in the biological responses of lung epithelial cells to cigarette smoke. *Biomarkers: biochemical indicators of exposure, response, and susceptibility to chemicals*, 14 (Suppl 1) (2009) 90–96.
- [7]. Stevenson CS, Docx C, Webster R, Battram C, Hynx D, Giddings J, Cooper PR, Chakravarty P, Rahman I, Marwick JA, Kirkham PA, Charman C, Richardson DL, Nirmala NR, Whittaker P, Butler K, Comprehensive gene expression profiling of rat lung reveals distinct acute and chronic responses to cigarette smoke inhalation. *American journal of physiology, Lung Cell. Mol. Physiol* 293 (2007) L1183–L1193.
- [8]. Izzotti A, Cartiglia C, Longobardi M, Balansky RM, D'Agostini F, Lubet RA, De Flora S, Alterations of gene expression in skin and lung of mice exposed to light and cigarette smoke, *Faseb J. Official Publ. Fed. Am. Soc. Exp. Biol* 18 (2004) 1559–1561.
- [9]. Gebel S, Gerstmayer B, Bosio A, Haussmann HJ, Van Miert E, Muller T, Gene expression profiling in respiratory tissues from rats exposed to mainstream cigarette smoke, *Carcinogenesis* 25 (2004) 169–178. [PubMed: 14578158]
- [10]. Hsu TC, Cherry LM, Bucana C, Shirley LR, Gairola CG, Mitosis-arresting effects of cigarette smoke condensate on human lymphoid cell lines, *Mutat. Res* 259 (1991) 67–78. [PubMed: 1988824]
- [11]. Li J, Tharappel JC, Han SG, Cantor AH, Lee EY, Gairola CG, Glauert HP, Effect of dietary selenium and cigarette smoke on pulmonary cell proliferation in mice, *Toxicol. Sci. Official J. Soc. Toxicol* 111 (2009) 247–253.
- [12]. Gairola CG, Howatt DA, Daugherty A, Dietary coenzyme Q10 does not protect against cigarette smoke-augmented atherosclerosis in apoE-deficient mice, *Free Radic. Biol. Med* 48 (2010) 1535–1539. [PubMed: 20227489]
- [13]. Han SG, Howatt DA, Daugherty A, Gairola CG, Atherogenic and pulmonary responses of ApoE- and LDL receptor-deficient mice to sidestream cigarette smoke, *Toxicology* 299 (2012) 133–138. [PubMed: 22659316]
- [14]. Kim J, Lee GR, Kim H, Jo YJ, Hong SE, Lee J, Lee HI, Jang YS, Oh SH, Lee HJ, Lee JS, Jeong W, Effective killing of cancer cells and regression of tumor growth by K27 targeting sulfiredoxin, *Free Radic. Biol. Med* 101 (2016) 384–392. [PubMed: 27825965]
- [15]. Jiang H, Wu L, Mishra M, Chawsheen HA, Wei Q, Expression of peroxiredoxin 1 and 4 promotes human lung cancer malignancy, *Am. J. Cancer Res* 4 (2014) 445–460. [PubMed: 25232487]
- [16]. Wei Q, Jiang H, Baker A, Dodge LK, Gerard M, Young MR, Toledano MB, Colburn NH, Loss of sulfiredoxin renders mice resistant to azoxymethane/dextran sulfate sodium-induced colon carcinogenesis, *Carcinogenesis* 34 (2013) 1403–1410. [PubMed: 23393226]



- [17]. Wu L, Jiang H, Chawsheen HA, Mishra M, Young MR, Gerard M, Toledano MB, Colburn NH, Wei Q, Tumor promoter-induced sulfiredoxin is required for mouse skin tumorigenesis, *Carcinogenesis* 35 (2014) 1177–1184. [PubMed: 24503444]
- [18]. Planson AG, Palais G, Abbas K, Gerard M, Couvelard L, Delaunay A, Baulande S, Drapier JC, Toledano MB, Sulfiredoxin protects mice from lipopolysaccharide-induced endotoxic shock, *Antioxidants Redox Signal.* 14 (2011) 2071–2080.
- [19]. Ticha JW, Ch., Rapid detection of toxic compounds in tobacco smoke condensates using high-resolution 1H-nuclear magnetic resonance spectroscopy, *Anal. Method* 8 (2016) 10.
- [20]. Woo HA, Jeong W, Chang TS, Park KJ, Park SJ, Yang JS, Rhee SG, Reduction of cysteine sulfinic acid by sulfiredoxin is specific to 2-cys peroxiredoxins, *J. Biol. Chem* 280 (2005) 3125–3128. [PubMed: 15590625]
- [21]. Wei Q, Jiang H, Matthews CP, Colburn NH, Sulfiredoxin is an AP-1 target gene that is required for transformation and shows elevated expression in human skin malignancies, *Proc. Natl. Acad. Sci. U. S. A* 105 (2008) 19738–19743. [PubMed: 19057013]
- [22]. Wei Q, Jiang H, Xiao Z, Baker A, Young MR, Veenstra TD, Colburn NH, Sulfiredoxin-Peroxiredoxin IV axis promotes human lung cancer progression through modulation of specific phosphokinase signaling, *Proc. Natl. Acad. Sci. U. S. A* 108 (2011) 7004–7009. [PubMed: 21487000]
- [23]. Kim H, Jung Y, Shin BS, Song H, Bae SH, Rhee SG, Jeong W, Redox regulation of lipopolysaccharide-mediated sulfiredoxin induction, which depends on both AP-1 and Nrf2, *J. Biol. Chem* 285 (2010) 34419–34428. [PubMed: 20826812]
- [24]. Soriano FX, Baxter P, Murray LM, Sporn MB, Gillingwater TH, Hardingham GE, Transcriptional regulation of the AP-1 and Nrf2 target gene sulfiredoxin, *Mol. Cell* 27 (2009) 279–282.
- [25]. Boettler U, Sommerfeld K, Volz N, Pahlke G, Teller N, Somoza V, Lang R, Hofmann T, Marko D, Coffee constituents as modulators of Nrf2 nuclear translocation and ARE (EpRE)-dependent gene expression, *JNB (J. Nutr. Biochem.)* 22 (2011) 426–440. [PubMed: 20655719]
- [26]. Arlt A, Sebens S, Krebs S, Geismann C, Grossmann M, Kruse ML, Schreiber S, Schafer H, Inhibition of the Nrf2 transcription factor by the alkaloid trigonelline renders pancreatic cancer cells more susceptible to apoptosis through decreased proteasomal gene expression and proteasome activity, *Oncogene* 32 (2013) 4825–4835. [PubMed: 23108405]
- [27]. Colburn NH, Bruegge WF, Bates JR, Gray RH, Rossen JD, Kelsey WH, Shimada T, Correlation of anchorage-independent growth with tumorigenicity of chemically transformed mouse epidermal cells, *Canc. Res* 38 (1978) 624–634.
- [28]. Freedman VH, Shin SI, Cellular tumorigenicity in nude mice: correlation with cell growth in semi-solid medium, *Cell* 3 (1974) 355–359. [PubMed: 4442124]
- [29]. Matsuyama M, Suzuki H, Strain differences in carcinogenesis by urethane administration to suckling mice with special reference to induction of lung cancer, *Br. J. Canc* 22 (1968) 527–532.
- [30]. Gurley KE, Moser RD, Kemp CJ, Induction of lung tumors in mice with urethane, *Cold Spring Harb. Protoc* 2015 (2015) pdb.prot077446.
- [31]. Festing MF, Yang A, Malkinson AM, At least four genes and sex are associated with susceptibility to urethane-induced pulmonary adenomas in mice, *Genet. Res* 64 (1994) 99–106. [PubMed: 7813906]
- [32]. Stakisaitis D, Mozuraite R, Kavaliauskaite D, Slekiene L, Balnyte I, Juodziukyniene N, Valanciute A, Sex-related differences of urethane and sodium valproate effects on Ki-67 expression in urethane-induced lung tumors of mice, *Exp. Therapeut. Med* 13 (2017) 2741–2750.
- [33]. Morozkova TS, Kaledin VI, Sex-related differences in the sensitivity to carcinogenic effect of urethane on the lungs in mice are reversed after neonatal androgenization, *Bull. Exp. Biol. Med* 159 (2015) 782–785. [PubMed: 26515180]
- [34]. Rhee SG, Woo HA, Kil IS, Bae SH, Peroxiredoxin functions as a peroxidase and a regulator and sensor of local peroxides, *J. Biol. Chem* 287 (2012) 4403–4410. [PubMed: 22147704]
- [35]. Rhee SG, Chae HZ, Kim K, Peroxiredoxins: a historical overview and speculative preview of novel mechanisms and emerging concepts in cell signaling, *Free Radic. Biol. Med* 38 (2005) 1543–1552. [PubMed: 15917183]

- [36]. Biteau B, Labarre J, Toledano MB, ATP-dependent reduction of cysteine-sulphinic acid by *S. cerevisiae* sulfiredoxin, *Nature* 425 (2003) 980–984. [PubMed: 14586471]
- [37]. Chang TS, Jeong W, Woo HA, Lee SM, Park S, Rhee SG, Characterization of mammalian sulfiredoxin and its reactivation of hyperoxidized peroxiredoxin through reduction of cysteine sulfinic acid in the active site to cysteine, *J. Biol. Chem* 279 (2004) 50994–51001. [PubMed: 15448164]
- [38]. Lowther WT, Haynes AC, Reduction of cysteine sulfinic acid in eukaryotic, typical 2-Cys peroxiredoxins by sulfiredoxin, *Antioxidants Redox Signal.* 15 (2011) 99–109.
- [39]. Field RW, Withers BL, Occupational and environmental causes of lung cancer, *Clin. Chest Med* 33 (2012) 681–703. [PubMed: 23153609]
- [40]. Ritchie KJ, Henderson CJ, Wang XJ, Vassieva O, Carrie D, Farmer PB, Gaskell M, Park K, Wolf CR, Glutathione transferase pi plays a critical role in the development of lung carcinogenesis following exposure to tobacco-related carcinogens and urethane, *Canc. Res* 67 (2007) 9248–9257.
- [41]. Balharry D, Sexton K, BeruBe KA, An in vitro approach to assess the toxicity of inhaled tobacco smoke components: nicotine, cadmium, formaldehyde and urethane, *Toxicology* 244 (2008) 66–76. [PubMed: 18082304]
- [42]. Hoffler U, El-Masri HA, Ghanayem BI, Cytochrome P450 2E1 (CYP2E1) is the principal enzyme responsible for urethane metabolism: comparative studies using CYP2E1-null and wild-type mice, *J. Pharmacol. Exp. Therapeut* 305 (2003) 557–564.
- [43]. Somers GI, Lindsay N, Lowdon BM, Jones AE, Freathy C, Ho S, Woodrooffe AJ, Bayliss MK, Manchee GR, A comparison of the expression and metabolizing activities of phase I and II enzymes in freshly isolated human lung parenchymal cells and cryopreserved human hepatocytes, *Drug Metab. Dispos* 35 (2007) 1797–1805. [PubMed: 17627976]
- [44]. Sheets PL, Yost GS, Carlson GP, Benzene metabolism in human lung cell lines BEAS-2B and A549 and cells overexpressing CYP2F1, *J. Biochem. Mol. Toxicol* 18 (2004) 92–99. [PubMed: 15122651]
- [45]. Schattenberg JM, Czaja MJ, Regulation of the effects of CYP2E1-induced oxidative stress by JNK signaling, *Redox Biol* 3 (2014) 7–15. [PubMed: 25462060]
- [46]. Reif AE, Heeren T, Consensus on synergism between cigarette smoke and other environmental carcinogens in the causation of lung cancer, *Adv. Canc. Res* 76 (1999) 161–186.
- [47]. Jayes L, Haslam PL, Gratziou CG, Powell P, Britton J, Vardavas C, Jimenez-Ruiz C, Leonardi-Bee J, SmokeHaz: systematic reviews and meta-analyses of the effects of smoking on respiratory health, *Chest* 150 (2016) 164–179. [PubMed: 27102185]
- [48]. Sun Y, Hegamy G, Colburn NH, Molecular cloning of five messenger RNAs differentially expressed in preneoplastic or neoplastic JB6 mouse epidermal cells: one is homologous to human tissue inhibitor of metalloproteinases-3, *Canc. Res* 54 (1994) 1139–1144.
- [49]. Matthews CP, Birkholz AM, Baker AR, Perella CM, Beck GR Jr., Young MR, Colburn NH, Dominant-negative activator protein 1 (TAM67) targets cyclooxygenase-2 and osteopontin under conditions in which it specifically inhibits tumorigenesis, *Canc. Res* 67 (2007) 2430–2438.
- [50]. Eferl R, Wagner EF, AP-1: a double-edged sword in tumorigenesis. *Nature reviews, Cancer* 3 (2003) 859–868. [PubMed: 14668816]
- [51]. Verde P, Casalino L, Talotta F, Yaniv M, Weitzman JB, Deciphering AP-1 function in tumorigenesis: fra-ternizing on target promoters, *Cell Cycle* 6 (2007) 2633–2639. [PubMed: 17957143]
- [52]. Singh A, Ling G, Suhasini AN, Zhang P, Yamamoto M, Navas-Acien A, Cosgrove G, Tudor RM, Kensler TW, Watson WH, Biswal S, Nrf2-dependent sulfiredoxin-1 expression protects against cigarette smoke-induced oxidative stress in lungs, *Free Radic. Biol. Med* 46 (2009) 376–386. [PubMed: 19027064]
- [53]. Wu CL, Yin JH, Hwang CS, Chen SD, Yang DY, Yang DI, c-Jun-dependent sulfiredoxin induction mediates BDNF protection against mitochondrial inhibition in rat cortical neurons, *Neurobiol. Dis* 46 (2012) 450–462. [PubMed: 22402332]
- [54]. Kim H, Lee GR, Kim J, Baek JY, Jo YJ, Hong SE, Kim SH, Lee J, Lee HI, Park SK, Kim HM, Lee HJ, Chang TS, Rhee SG, Lee JS, Jeong W, Sulfiredoxin inhibitor induces preferential death

of cancer cells through reactive oxygen species-mediated mitochondrial damage, *Free Radic. Biol. Med* 91 (2016) 264–274. [PubMed: 26721593]

- [55]. Stathopoulos GT, Sherrill TP, Cheng DS, Scoggins RM, Han W, Polosukhin VV, Connelly L, Yull FE, Fingleton B, Blackwell TS, Epithelial NF-kappaB activation promotes urethane-induced lung carcinogenesis, *Proc. Natl. Acad. Sci. U. S. A* 104 (2007) 18514–18519. [PubMed: 18000061]

Author Manuscript

Author Manuscript

Author Manuscript

Author Manuscript

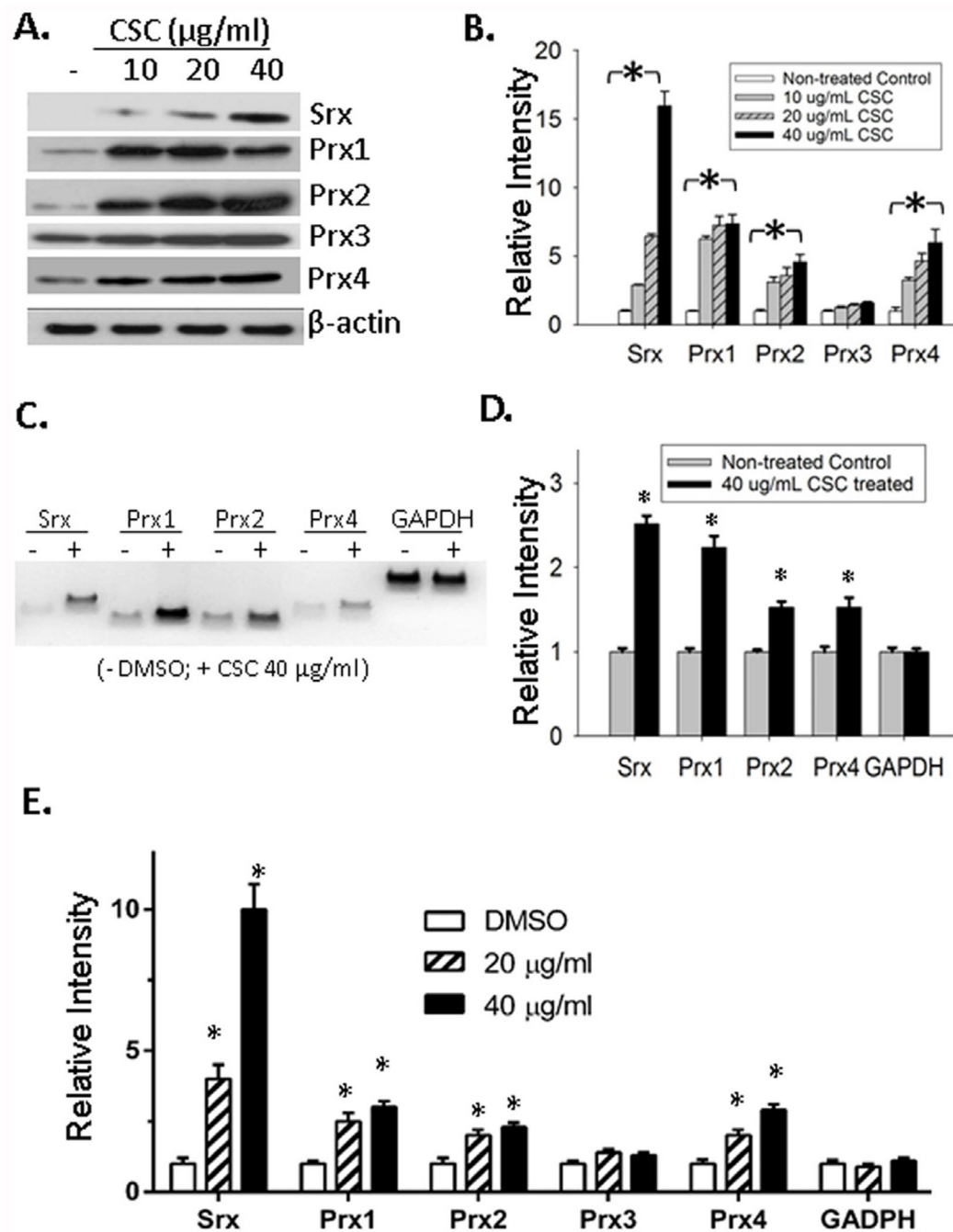


**Fig. 1.** CSC activated the expression of SrX and certain members of the Prxs in BEAS2B cells. (A) Representative western blot results of SrX and Prxs in cells treated with CSC or vehicle DMSO at indicated concentration for 48 h. (B) Bands shown in (A) were quantitated and relative intensity was adjusted using the ratio to β-actin. Data from three independent experiments were analyzed. \**p* < 0.05 (n = 3, one way ANOVA). (C) Representative results of reverse transcription PCR to examine the mRNA levels of SrX and Prxs in control and CSC treated cells. (D) Bands shown in (C) were quantitated and relative intensity was adjusted using the ratio to GAPDH. Data from three independent experiments were

analyzed. \* $p < 0.05$  ( $n = 3$ ,  $t$ -test). (E) The levels of specified mRNA were measured using quantitative real-time PCR and data from six repeats were analyzed. \*Compared with DMSO control,  $p < 0.05$  ( $n = 6$ , one way ANOVA).

Author Manuscript

Author Manuscript

Author Manuscript

Author Manuscript

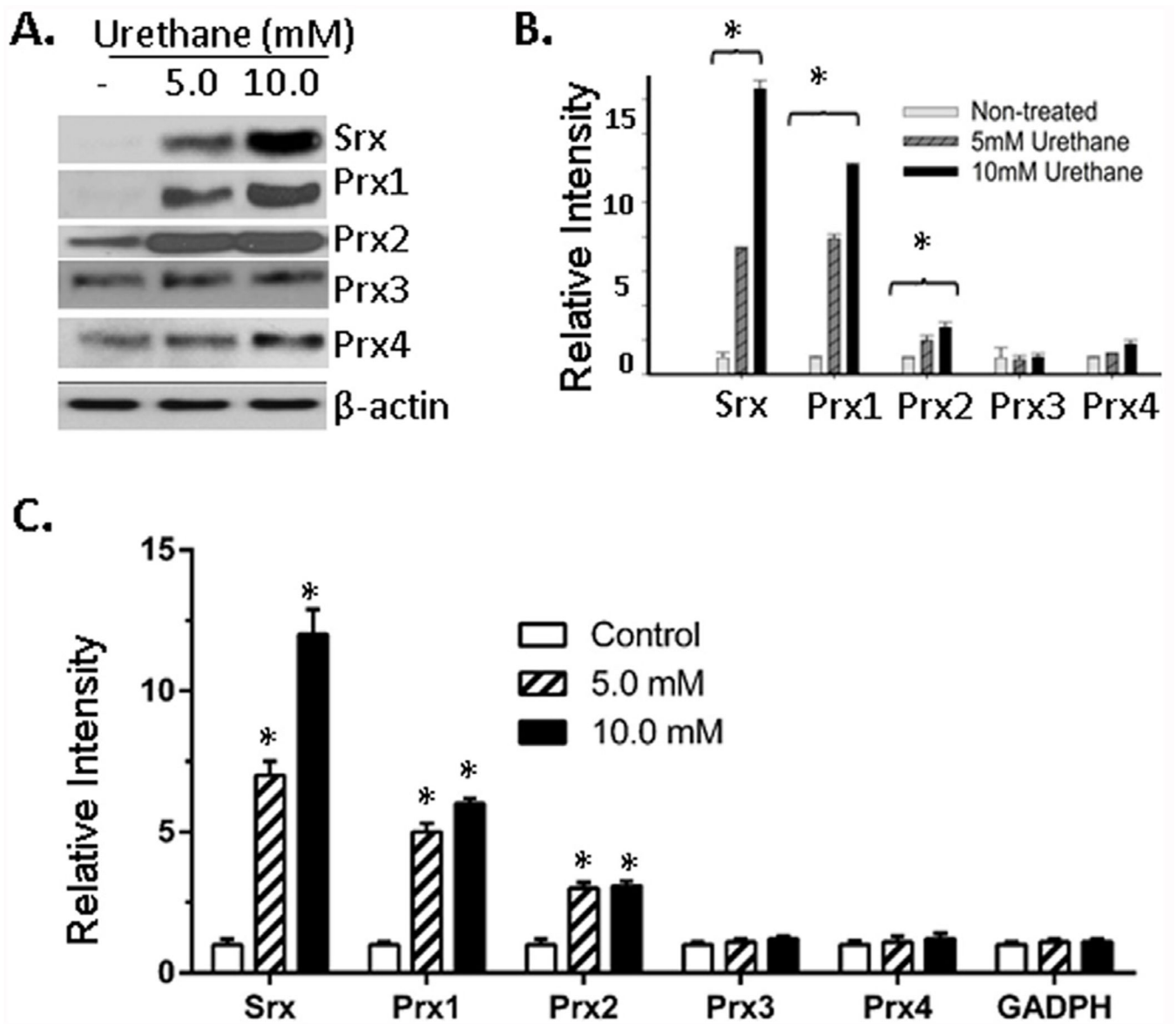


**Fig. 2. Urethane activated the expression of Srx and certain Prxs in BEAS2B cells.** (A) Representative western blot results of Srx and Prxs in cells treated with urethane or vehicle saline at indicated concentration for 48 h. (B) Bands shown in (A) were quantitated and relative intensity was adjusted using the ratio to  $\beta$ -actin. Data from three independent experiments were analyzed. (C) Quantitative real-time PCR was used to measure the levels of specified mRNA. Data from six repeats were analyzed. \*Compared with control,  $p < 0.05$  ( $n = 3$  in B and  $n = 6$  in C, one way ANOVA).



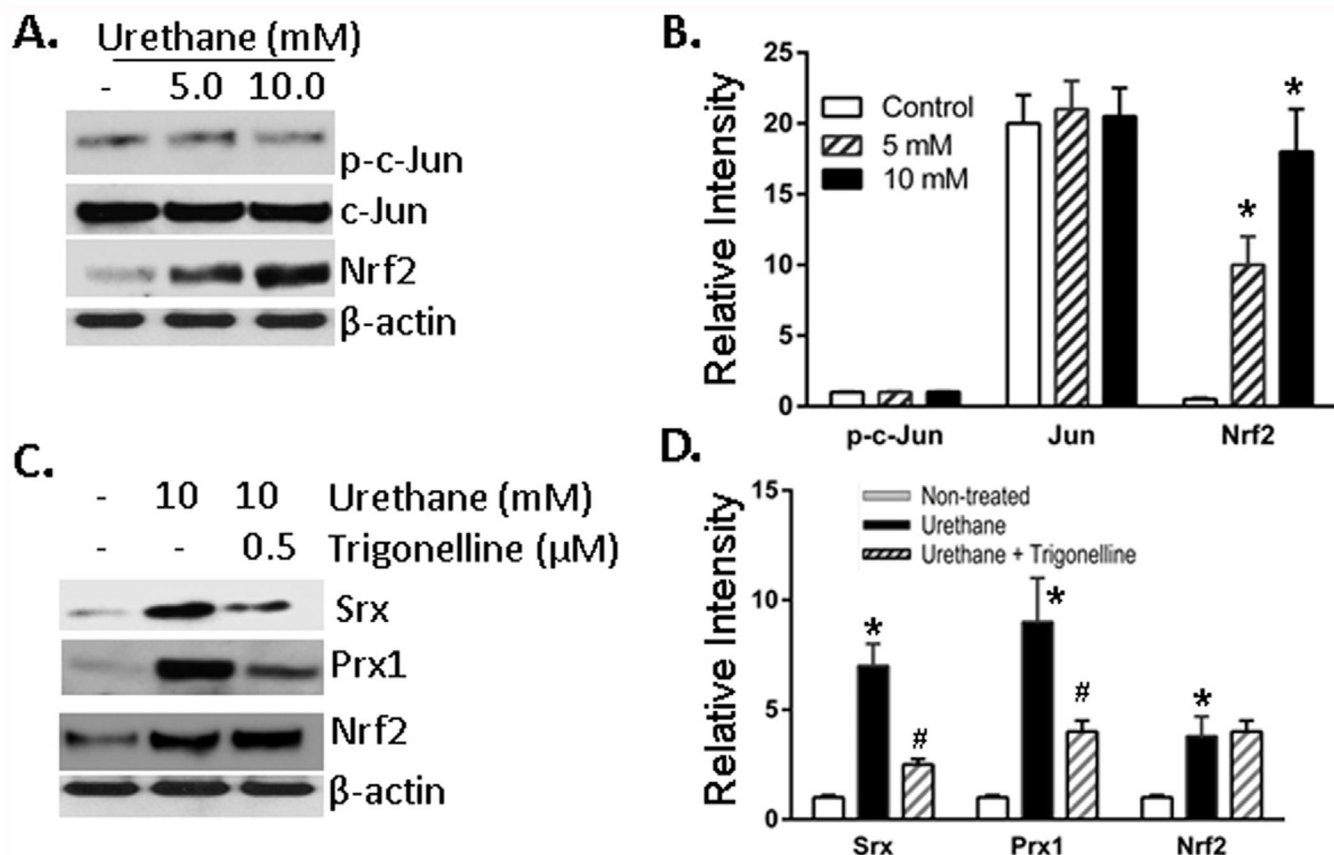


**Fig. 3. Urethane stimulated the expression of Srx and Prx1 in BEAS2B cells through the activation of Nrf2 in BEAS2B cells.**

(A) Representative western blot results showed increased expression of Nrf2 but not c-Jun in cells treated with urethane at indicated concentration for 48 h. (B) Bands shown in (A) were quantitated and relative intensity was adjusted using the ratio to  $\beta$ -actin. Data from three independent experiments were analyzed. \* $p < 0.05$  ( $n = 3$ , one way ANOVA). (C) Representative western blot results showed that the expression of Srx and Prx1 was inhibited by the presence of trigonelline (a specific inhibitor of Nrf2). Cells were treated with urethane in the presence or absence of trigonelline for 48 h. (D) Bands shown in (C) were quantitated and relative intensity was adjusted using the ratio to  $\beta$ -actin. Data from three independent experiments were analyzed. \*Compared with control,  $p < 0.05$ ; #compared with urethane treated group,  $p < 0.05$  ( $n = 3$ , two way ANOVA).

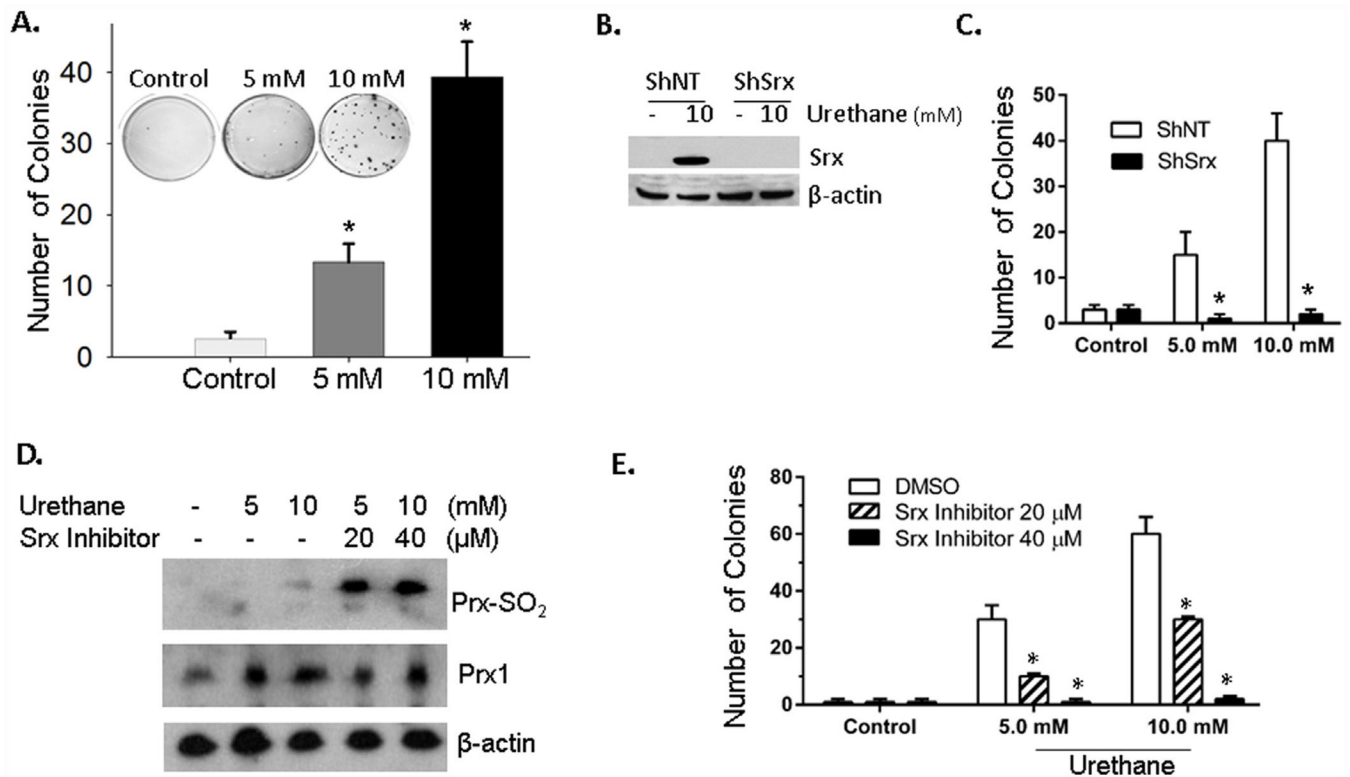


**Fig. 4. SrX contributed to urethane-induced BEAS2B cell transformation.**

(A) Representative images and data of anchorage independent colony growth showed that urethane but not saline increased the number of colonies in soft agar. \*Compared with control,  $p < 0.05$  ( $n=6$ , one-way ANOVA). (B) Cells stably expressing a non-target ShRNA (ShNT) or ShRNA targeting SrX (ShSrx) were treated with saline or urethane. Western blot results showed efficient knockdown of SrX in urethane treated cells. (C) ShNT or ShSrx cells were cultured in the presence of urethane in soft agar and anchorage independent colonies were examined. \*Compared with ShNT,  $p < 0.05$  ( $n = 6$ , two way ANOVA). (D) Cells were treated with indicated concentration of urethane in the absence or presence of K27 (a specific inhibitor of SrX) for 24 h. Cells were harvested and the levels of hyperoxidized Prxs were examined. (E) Anchorage independent colony growth of cells treated with saline or urethane in the presence or absence of K27 at indicated concentration. \*Compared with DMSO,  $p < 0.05$  ( $n = 6$ , two way ANOVA).

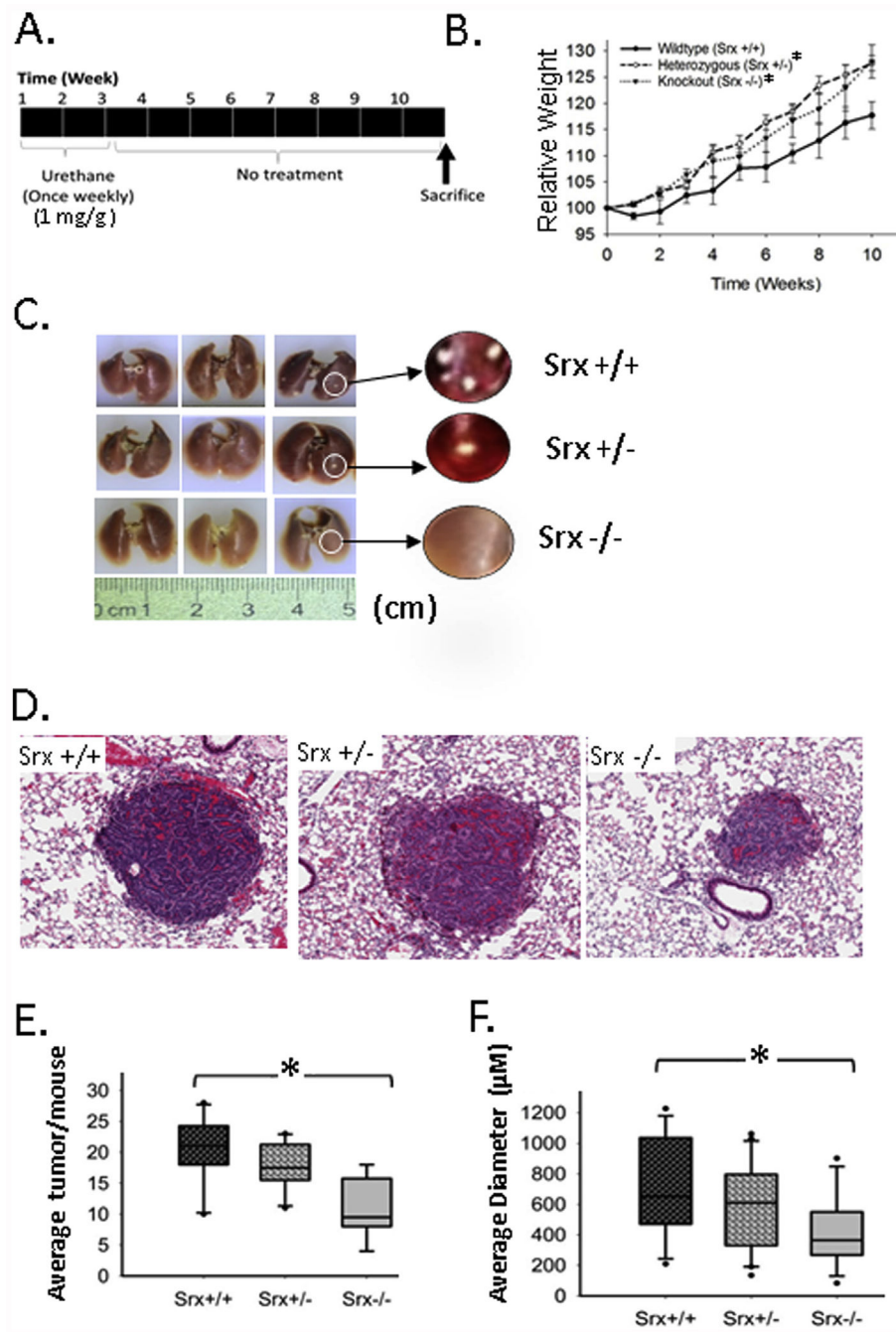


**Fig. 5. SrX knockout mice were resistant to urethane-induced lung tumorigenesis.** (A) Schematic presentation of the urethane-induced mouse lung tumorigenesis protocol; (B) Effect of urethane on the body weight of treated mouse groups with different genotypes (SrX wildtype, +/+; heterozygous, +/-; knockout, -/-). \*Compared with SrX +/+,  $p < 0.05$  ( $n = 15$ , paired  $t$ -test). (C) Representative gross images of extracted lungs showed visible tumors on the surface. (D) Representative microscopic images of lung tumors in H&E staining. (E) The average number of lung tumors in mice with different genotypes was compared; (F) The

average size of lung tumors in mice with different genotypes was compared. \*Compared with  $Srx+/+$ ,  $p < 0.05$  ( $n = 15$ ,  $t$ -test in both E and F).

Author Manuscript

Author Manuscript

Author Manuscript

Author Manuscript

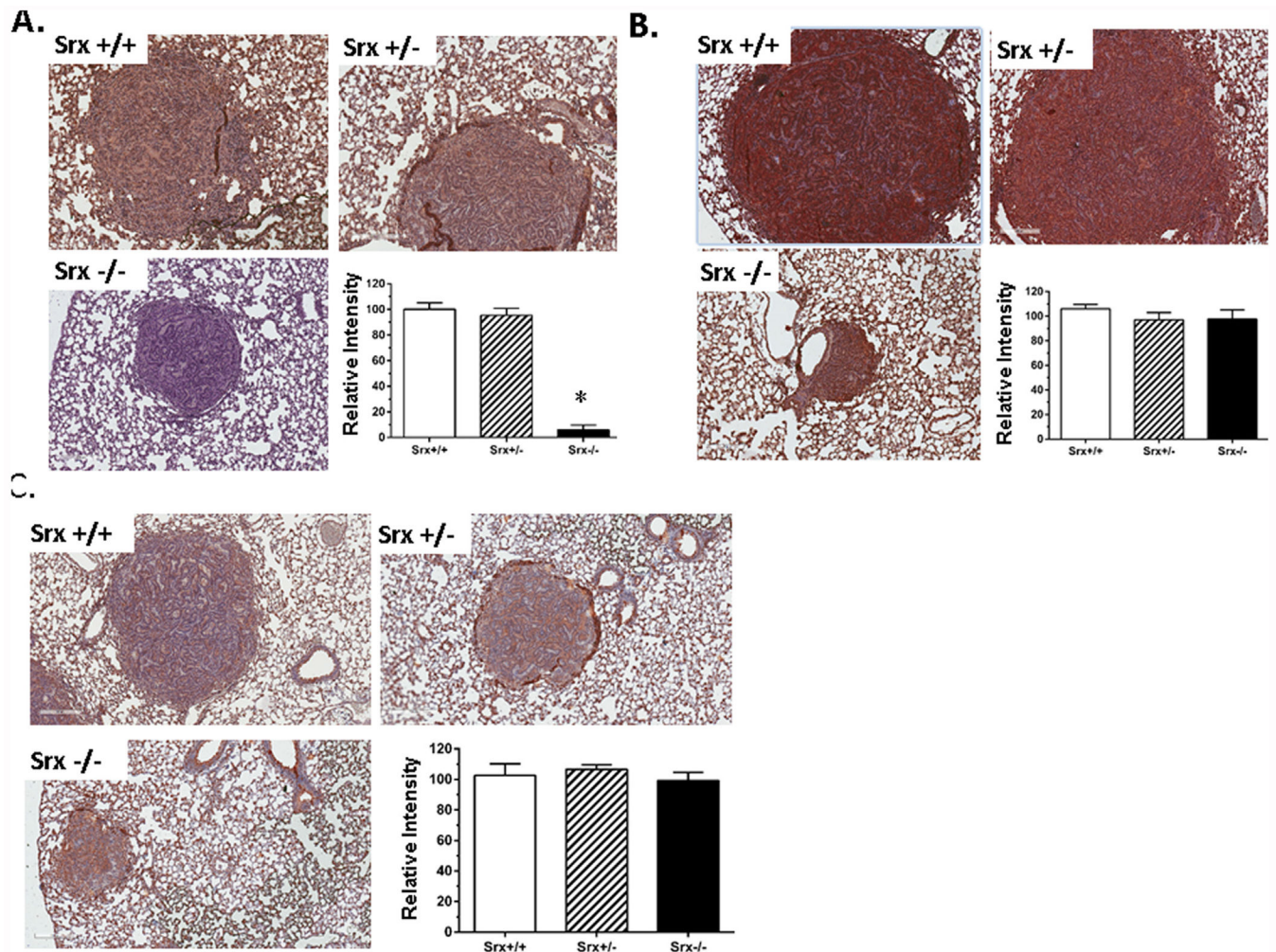


**Fig. 6. The expression of Prx1 and Nrf2 in urethane-induced mouse lung tumors was not affected by the loss of SrX.**

(A) Anti-Srx staining of representative mouse tumors from different genotypes and the quantitation of staining intensity. \*Compared with *Srx*<sup>+/+</sup>,  $p < 0.05$  ( $n = 5$ ,  $t$ -test). (B) Anti-Prx1 staining of representative mouse tumors from different genotypes and the quantitation of staining intensity. (C) Anti-Nrf2 staining of representative mouse tumors from different genotypes and the quantitation of staining intensity. Note that there's no statistically significant difference in the average of Prx1/Nrf2 staining intensity in tumors from different genotypes.



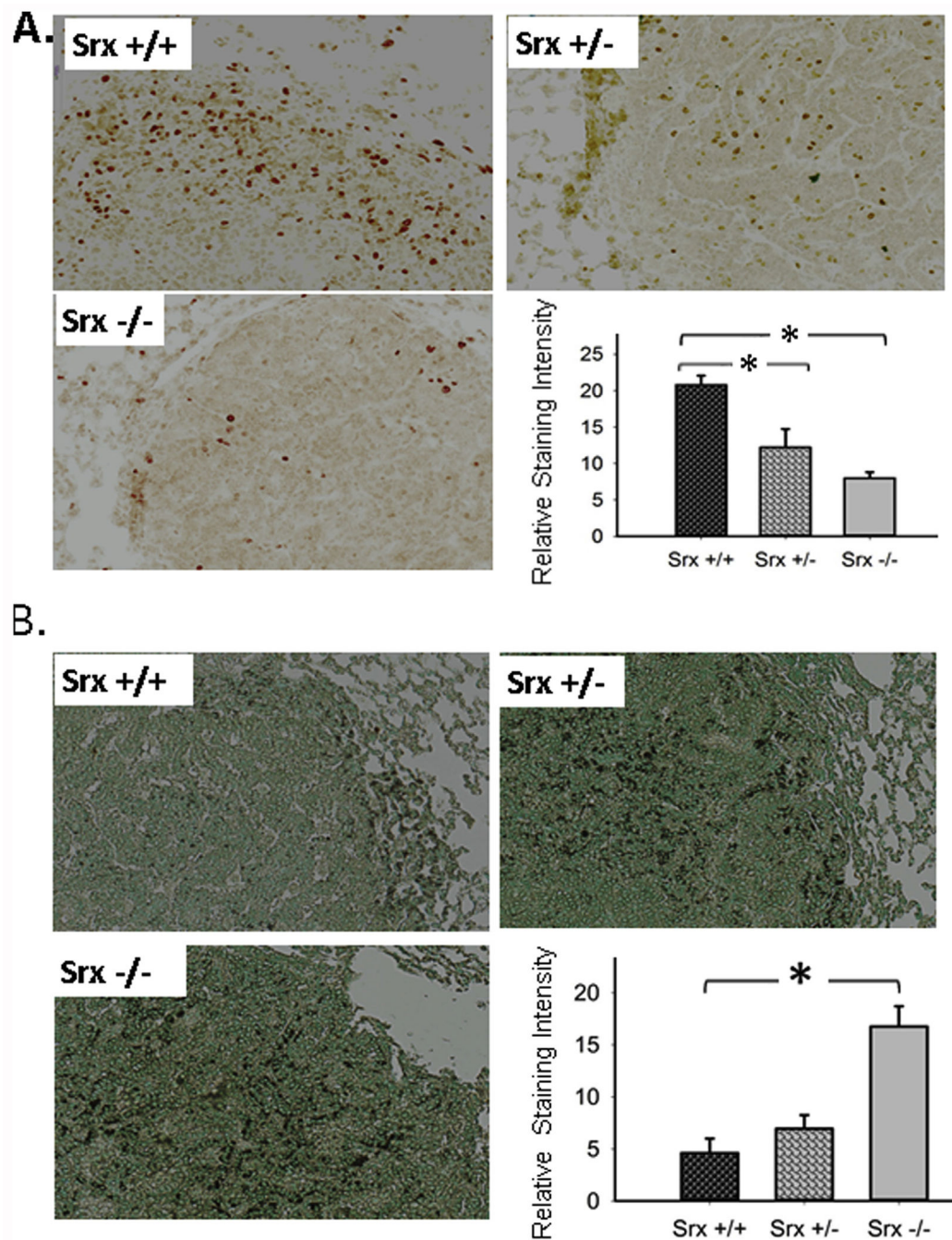


**Fig. 7. Depletion of Srx decreased the rate of cell proliferation and increased apoptosis in urethane-induced mouse lung tumors.**

(A) Anti-Ki67 staining of representative lung tumors from mice with different genotypes and the quantitation of staining intensity. (B) TUNEL staining of representative lung tumors from mice with different genotypes and the quantitation of staining intensity. \*Compared with Srx<sup>+/+</sup>,  $p < 0.05$  ( $n = 5$ ,  $t$ -test in both A and B).